Inorganica Chimica Acta 429 (2015) 183–188

Contents lists available at ScienceDirect

Inorganica Chimica Acta

journal homepage: www.elsevier.com/locate/ica

Nitric oxide reactivity of a manganese(II) complex leading to nitrosation of the ligand

Aswini Kalita, Somnath Ghosh, Biplab Mondal *

Department of Chemistry, Indian Institute of Technology Guwahati, Assam 781039, India

ARTICLE INFO

Article history:
Received 9 October 2014
Received in revised form 11 December 2014
Accepted 12 December 2014
Available online 14 February 2015

Keywords:
Manganese(II) complex
Nitric oxide
Reduction of metal center
Ligand nitrosation

ABSTRACT

Manganese(II) complexes, $[Mn(L)(Cl)_2]$, **1** and $[Mn(L)(H_2O)_2](ClO_4)_2$, **2** {L = N^1,N^2-bis((pyridine-2-yl)methyl)ethane-1,2-diamine} were prepared and characterized. In acetonitrile solution, complex **1** did not react with nitric oxide gas. However, addition of nitric oxide gas to the acetonitrile solution of complex **2** resulted in unstable Mn(II)-nitrosyl intermediate. The formation of nitrosyl intermediate was evidenced by UV–Vis, solution FT-IR, ^{1}H NMR spectral studies. Subsequently, Mn(II) center in the complex **2** was undergone reduction to Mn(I) with a simultaneous N-nitrosation of the ligand. The N-nitrosated ligand was isolated and characterized. It should be noted that the corresponding Cu(II) complex of the same ligand in presence of nitric oxide was not found to yield Cu(II)-nitrosyl.

1. Introduction

The reactions of nitric oxide (NO) with transition metal ions and formation of metal-nitrosyls have long been of interest because of their relevance and importance in biological systems [1–5]. Many of the physiological events of NO are attributed to the formation of nitrosyls of metalloproteins [6–8]. For instance, metal-nitrosyl adducts are believed to play important roles in nitrosation reactions of various thiols to result in S-nitrosothiols which are proposed as carriers of NO equivalents in cellular systems [9–11]. On the other hand, the reduction of metal ion by NO has been known for a long time. For example, ferriheme proteins are known to undergo reduction to ferroheme in presence of NO through Fe(III)-nitrosyl intermediate. In this direction, iron-nitrosyls, both in protein and synthetic model systems have been studied extensively [12–17]. The reduction of Cu^{II} centres in some proteins, such as cytochrome *c* oxidase and laccase, by NO is known for a long time [18,19]. In recent years this has been exemplified by a number of model copper(II) complexes [20–28].

The examples manganese-nitrosyls in organometallic, porphyrin and thalocyanine complexes are known; however, the detail reactivity of manganese complexes with NO has not been studied to that extent [29–32]. A few Mn(II)-nitrosyls are reported recently with an aim to develop NO releasing material for photo dynamic therapy [33,34]. Other than those, Mascharak et al. reported the reductive nitrosylation of the metal ion in the reaction of a μ-oxo bridged Mn(III) complex with NO [35].

In our laboratory, we have been studying the reactivity of NO with copper(II) complexes and found the reduction of metal ion by NO leads to the N-nitrosation and diazotization at the secondary and primary amine centers, respectively, of ligand frameworks [24–28]. Interestingly, the N-nitrosation, in cases of Cu(II) complexes, may not necessarily always proceed through Cu(II)-nitrosyl formation. Depending upon the ligand denticity and geometry of the complex, it may proceed through a deprotonation mechanism in presence of base. For example, in case of tetradentate tripodal ligand, the N-nitrosation takes place through a Cu(II)-nitrosyl intermediate [25]. In case of tetradentate macrocyclic ligand, it proceeds through a deprotonation of the N-H group [36]. This diversity of the mechanistic pathway actually prompted us to study the NO reactivity of Mn(II) complexes.

For the present study, a tetradentate N-donor ligand, L {L = N^1,N^2-bis((pyridine-2-yl)methyl)ethane-1,2-diamine} having two pyridine nitrogen and two aliphatic amine nitrogen is chosen (Fig. 1). Earlier, NO reactivity of Cu(II) complex of the same ligand has been reported from our laboratory. So the present study will also demonstrate the difference of reactivity towards NO while moving from Cu(II) to Mn(II).

2. Experimental

2.1. Materials and methods

All reagents and solvents of reagent grade were purchased from commercial sources and used as received except specified. Acetonitrile was distilled from calcium hydride. Deoxygenation of

* Corresponding author. Tel.: +91 361 258 2317; fax: +91 361 258 2339.
E-mail address: biplab@iitg.ernet.in (B. Mondal).

http://dx.doi.org/10.1016/j.ica.2014.12.040
0020-1693/

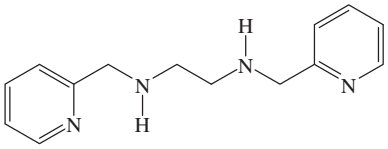

Fig. 1. Ligand (**L**) used for the present study.

the solvent and solutions was effected by repeated vacuum/purge cycles or bubbling with argon for 30 min. Nitric oxide gas was purified by passing it through a KOH and P_2O_5 column. UV–Vis spectra were recorded on a Perkin–Elmer LAMBDA 35 UV–Vis spectrophotometer. FT-IR spectra of the samples were taken on a Perkin Elmer spectrophotometer with samples prepared either as KBr pellets or in a KBr cell. Solution electrical conductivity was measured using a Systronic 305 conductivity bridge. ^{1}H NMR spectra were recorded in a 400 MHz Varian FT spectrometer. Chemical shifts (ppm) were referenced either with an internal standard (Me_4Si) or to the residual solvent peaks. The X-band Electron Paramagnetic Resonance (EPR) spectra were recorded on a JES-FA200 ESR spectrometer, at room temperature and 77 K with microwave power, 0.998 mW; microwave frequency, 9.14 GHz and modulation amplitude, 2. Elemental analyses were obtained from a Perkin Elmer Series II Analyzer. The magnetic moment of complex was measured on a Cambridge Magnetic Balance.

Single crystals were grown by slow diffusion followed by slow evaporation technique. The intensity data were collected using a Bruker SMART APEX-II CCD diffractometer, equipped with a fine focus 1.75 kW sealed tube MoK_α radiation ($\lambda = 0.71073$ Å) at 273(3) K, with increasing ω (width of 0.3° per frame) at a scan speed of 3 s/frame. The SMART software was used for data acquisition [37]. Data integration and reduction were undertaken with SAINT and XPREP software [38]. Structures were solved by direct methods using SHELXS-97 and refined with full-matrix least squares on F^2 using SHELXL-97 [39]. Structural illustrations have been drawn with ORTEP-3 for Windows [40].

2.2. Experimental

2.2.1. Synthesis of *L*

The ligand **L** was reported earlier [41]. To a solution of pyridine-2-carboxaldehyde (2.14 g, 20 mmol) in 20 ml methanol, ethylenediamine (0.60 g, 10 mmol) was added into a 50 ml round bottom flask equipped with a stirring bar. The solution was refluxed for 5 h. The resulting reddish-yellow solution was then reduced by $NaBH_4$ (1.52 g, 40 mmol). Removal of the solvent under reduced pressure affords a crude mass. It was dissolved in water (50 ml) and extracted with chloroform (50 ml × 4 portions). The organic part was dried under reduced pressure and the reddish yellow oil thus obtained was subjected to chromatographic purification using a silica gel column to yield the pure ligand, **L** as yellow oil. Yield: 80%, 1.96 g. UV–Vis (acetonitrile): λ_{max}, 241 nm (ε, 20335 M^{-1} - cm^{-1}). FT-IR in KBr: 2791, 1591, 1475, 1431, 767 cm^{-1}. ^{1}H NMR (400 MHz, $CDCl_3$) δ_{ppm}: 2.81 (s, 4H), 3.91 (s, 4H), 7.12–7.15 (t, 2H), 7.30 (d, 4H) 7.60–7.64 (t, 2H), 8.52–8.53 (d, 2H). ^{13}C NMR (100 MHz, $CDCl_3$) δ_{ppm}: 46.9, 53.1, 120.5, 120.8, 134.4, 147.5 and 157.8. ESI-Mass (m+1), Calc. 243.32. Found: 243.04.

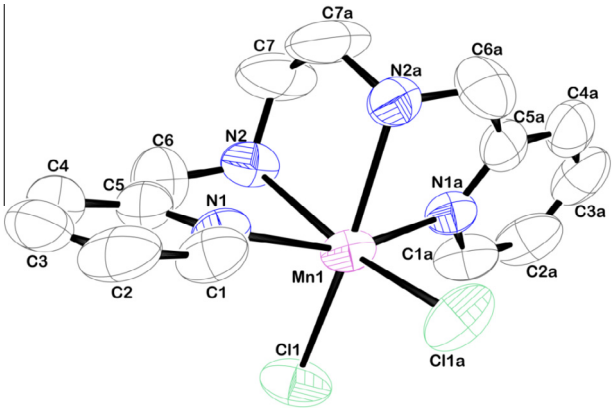

Fig. 2. ORTEP diagram of complex **1** (50% thermal ellipsoid plot; H-atoms are removed for clarity).

2.2.2. Synthesis of complex *1*

$[Mn^{II}(H_2O)_4]Cl_2$ (0.989 g, 5 mmol) was dissolved in 10 ml of distilled methanol. To this solution, **L** (1.21 g, 5 mmol), dissolved in distilled methanol was added slowly with constant stirring. The color of the solution turned into pale-yellow. The stirring was continued for 2 h at room temperature. The volume of the solution was then reduced to ~2 ml. To this, diethyl ether (10 ml) was added to layer on it and kept overnight in a freezer. This resulted into yellow colored precipitate of complex **1**. Yield: 1.58 g (~85%) and UV–Vis (methanol): λ_{max}, 474 nm (ε, 380 M^{-1} cm^{-1}), 595 nm (ε, 201 M^{-1} - cm^{-1}). ^{1}H NMR (400 MHz, CD_3OD) δ_{ppm}: 1.33 (s, 4H), 2.52 (s, 4H), 8.67 (s, 4H), 9.10 (s, 2H), 9.86 (s, 2H). X-band EPR (in methanol at RT) g_{av} = 2.025. FT-IR (KBr pellet): 3429, 3270, 3232, 2884, 1604, 1569, 1481, 1431, 1264, 1095, 1008, 775, 637 cm^{-1}. μ_{obs}, 5.82 BM.

2.2.3. Synthesis of complex *2*

Complex **1** (0.736 g, 2 mmol) was dissolved in minimum volume of acetonitrile. To this, aqueous solution of silver nitrate (0.680 g, 4 mmol; 2 ml) was added with constant stirring. The precipitated AgCl was removed by filtration through a frit. To the filtrate, aqueous solution of sodium perchlorate (20%, 2 ml) was added dropwise and the mixture was kept in freezer for 12 h which afforded brown precipitate of complex **2**. Yield, 595 mg (~60%).

The complex **2** can also be prepared from manganese(II) perchlorate, hexahydrate. $[Mn^{II}(H_2O)_6](ClO_4)_2$. It (1.81 g, 5 mmol) was dissolved in 10 ml of distilled acetonitrile. To this solution, **L** (1.21 g, 5 mmol) was added slowly with constant stirring. The color of the solution turned into brown. The stirring was continued for 2 h at room temperature. The volume of the solution was then reduced to 2 ml. To this, benzene (5 ml) was added to layer on it and kept overnight in a freezer. This resulted in brown colored precipitate of complex **2**. Yield: 2.44 g (82%) and UV–Vis (acetonitrile): λ_{max}, 246 nm (ε, 7108 M^{-1} cm^{-1}), λ_{max}, 296 nm (ε, 8345 M^{-1} cm^{-1}), λ_{max}, 421 nm (ε, 1620 M^{-1} cm^{-1}), 644 nm (ε, 210 M^{-1} cm^{-1}). X-band EPR (in acetonitrile at RT: g_{av} = 2.021. FT-IR (KBr pellet):

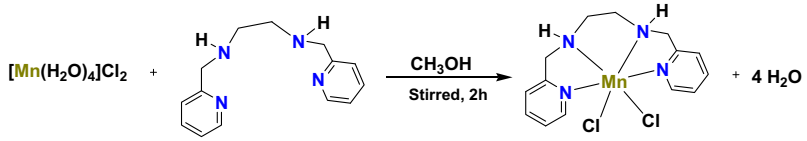

Scheme 1. Synthesis of complex **1**.

Table 1
Crystallographic data for complex **1**.

	Complex **1**
Formula	$C_{14}H_{16}Mn_1N_4Cl_2$
Mol. wt.	366.15
Crystal system	orthorhombic
Space group	Aba2
T (K)	296(2)
Wavelength (Å)	0.71073
a (Å)	15.6763(17)
b (Å)	12.2746(12)
c (Å)	8.5407(12)
α (°)	90.00
β (°)	90.00
γ (°)	90.00
V (Å^3)	1643.4(3)
Z	4
Density (mg m^{-3})	1.480
Absorption coefficient (mm^{-1})	1.126
Absorption correction	none
F(000)	748
Total no. of reflections	1122
Reflections, $I > 2\sigma(I)$	934
Maximum 2θ (°)	25.24
Ranges (h, k, l)	$-18 \leqslant h \leqslant 17$ $-14 \leqslant k \leqslant 13$ $-10 \leqslant l \leqslant 5$
Complete to 2θ (%)	98.7
Refinement method	full-matrix least-squares on F^2
GOF (F^2)	0.999
R indices [$I > 2\sigma(I)$]	0.0354
R indices (all data)	0.1014

Table 2
Selected bond length (Å) of complex **1**.

	Bond length (Å)
Mn1–Cl1	2.471(2)
Mn1–N1	2.271(5)
Mn1–N2	2.328(4)
N1–C1	1.338(7)
N1–C5	1.339(7)
N2–C6	1.455(8)
N2––C7	1.441(9)
C1–C2	1.384(9)
C2–C3	1.37(1)
C3–C4	1.37(1)
C4–C5	1.370(9)
C5–C6	1.529(8)

Table 3
Selected bond angles (°) of complex **1**.

	Bond angle (°)
Cl1–Mn1–N1	96.1(1)
Cl1–Mn1–N2	91.3(1)
N1–Mn1–N2	73.2(1)
N1–Mn1–Cl1	96.1(1)
N2–Mn1–Cl1	91.3(1)
Mn1–N1–C1	124.3(3)
Mn1–N1–C5	117.2(3)
C1–N1–C5	118.2(4)
Mn1–N2–C6	110.6(3)
Mn1–N2–C7	108.3(4)

3314, 3234, 2885, 1612, 1440, 1314, 1148, 1091, 930, 770, 626 cm^{-1}. Molar conductivity in acetonitrile, Λ_M (S cm^{-1}), 124. μ_{obs}, 5.76 BM. Mass {[MnL(ClO$_4$)]$^+$}, Calc. 396.0397. Found: 396.0361.

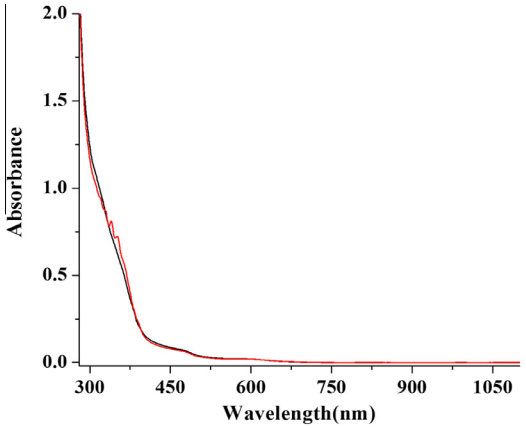

Fig. 3. UV–Vis spectra of complex **1** (black trace), after purging NO (red trace) in acetonitrile. (For interpretation of the references to color in this figure legend, the reader is referred to the web version of this article.)

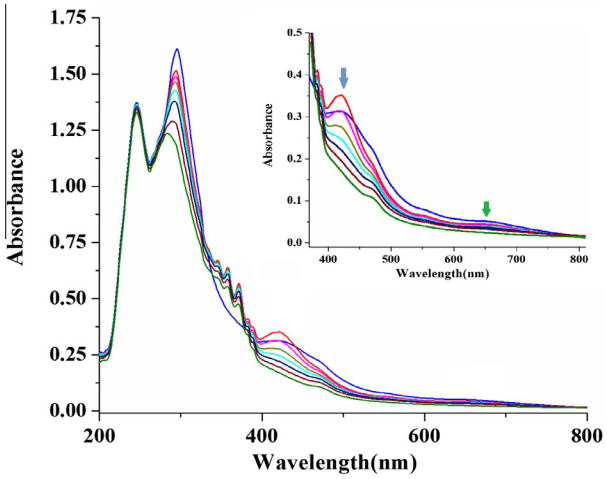

Fig. 4. UV–Vis spectrum of complex **2** (blue trace), after purging NO to complex **2** (red trace) and gradual diminishing of peaks at 421 nm and 644 nm with time in acetonitrile. Inset shows the spectral change in the range from 350 nm to 800 nm. (For interpretation of the references to color in this figure legend, the reader is referred to the web version of this article.)

2.3. Isolation of modified ligand **L′**

Complex **2** (0.992 g, 2.0 mmol) was dissolved in 10 ml of distilled and degassed acetonitrile. To this solution NO gas was purged for 1 min. After removing the excess NO by several cycles of vacuum purge, the resulting yellowish solution was allowed to stand at room temperature for 1 h. A light pink colored precipitate was formed which was then separated by filtration under argon and the filtrate was dried over vacuum. The crude mixture was then purified by column chromatography to get pure ligand **L** as yellow oil and **L′**-perchlorate as light yellow solid. Yield; **L**: 95 mg (30%) and **L′**-perchlorate: 146 mg (40%). FT-IR (KBr pellet): 3408, 2928, 1668, 1592, 1571, 1457, 1436, 1355, 1151, 1118, 1093, 998, 758, 614 cm^{-1}. ESI-Mass (m+1), Calc. 301.1335. Found: 301.1287. ^{1}H NMR (400 MHz, CDCl$_3$) δ_{ppm}: 4.19–4.21 (t, 1H), 4.56–4.58 (t, 1H), 5.00 (s, 2H), 5.05 (s, 1H), 5.14 (s, 2H), 5.82 (s, 1H), 7.81–7.83 (d, 1H), 7.91–7.98 (m, 3H), 8.47–8.51 (m, 3H), 8.73–8.75 (d, 1H). ^{13}C NMR (100 MHz, CDCl$_3$) δ_{ppm}: 46.0, 50.5, 124.9, 125.4, 142.3, 145.7 and 156.1.

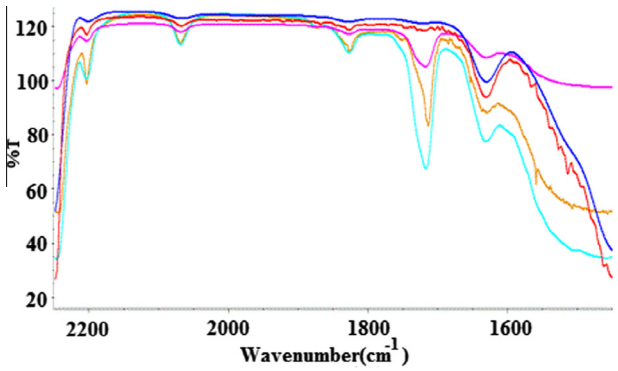

Fig. 5. FT-IR spectra of complex **2** after purging NO (green trace) and gradual decay of the peak at 1718 cm^{-1} in acetonitrile. (For interpretation of the references to color in this figure legend, the reader is referred to the web version of this article.)

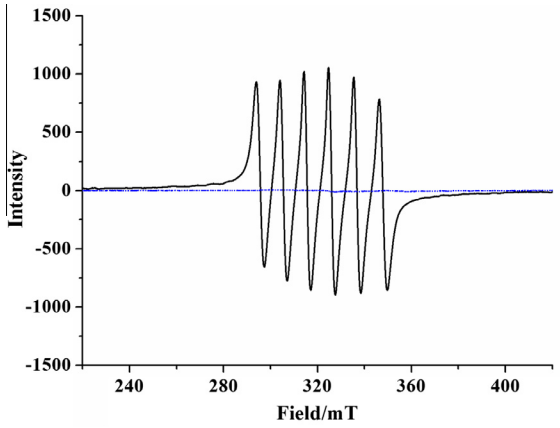

Fig. 6. X-band EPR spectra of complex **2** before (black trace) and after (blue trace) the reaction with NO in acetonitrile at room temperature. (For interpretation of the references to color in this figure legend, the reader is referred to the web version of this article.)

3. Results and discussion

The ligand was prepared using a reported protocol from the reaction of ethylenediamine with two equivalent of pyridine-2-carboxaldehyde followed by reduction of the corresponding imine using $NaBH_4$ (Section 2) [41]. The ligand was characterized by various spectroscopic techniques (Section 2). Complex **1** was prepared from the reaction of manganese(II) chloride, tetrahydrate with equivalent amount of ligand, **L** in methanol solution (Scheme 1). The complex was characterized by various spectroscopic methods as well as single crystal X-ray structure determination. The ORTEP view of complex **1** is shown in Fig. 2. Crystallographic data, important bond angles and distances are listed in Tables 1–3, respectively. The crystal structure reveals a distorted octahedral geometry around the central metal ion. Four nitrogen atoms from the ligand and two chlorine atoms are coordinated to the Mn(II) center. The Cl atoms are coordinated in *cis*-geometry. The Mn-N_{py} and Mn-N_{amine} distances are 2.271 and 2.328 Å, respectively. The average Mn-Cl distance is 2.471 Å. These are within the range of reported complexes. The complex **1** displays characteristic EPR signal in X-band (Supporting information).

In acetonitrile solution, it shows d-d transition at 595 nm along with intra ligand transitions at in UV-region (Supporting information).

Addition of nitric oxide gas in dry and degassed acetonitrile solution of complex **1** was not found to result in any change. This has been monitored by UV–Vis spectroscopy (Fig. 3). This is perhaps because of strong coordination of chloride ion with Mn(II).

To study further, the chloride ions in complex **1** are replaced by water to afford complex **2**. This has been done by treating the acetonitrile solution of complex **1** with aqueous silver nitrate followed by addition of saturated aqueous sodium perchlorate solution (Section 2). The complex **2** can also be prepared by stirring a mixture of manganese(II) perchlorate, hexahydrate with equivalent amount of ligand in acetonitrile under argon atmosphere (Section 2). It was characterized by spectral analyses and microanalysis (Section 2). In positive mode ESI mass spectrum, a peak at 396.0361 was observed which corresponds to $[MnL(ClO_4)]^+$ (Calculated, 396.0397). Even after several attempts, an X-ray quality single crystal of the complex has not been grown.

Complex **2** in acetonitrile solution absorbs at 644 nm in the UV–Vis spectrum (Fig. 4). Addition of NO gas into the degassed acetonitrile solution of complex **2** resulted in the appearance of a new band at 421 nm (Fig. 4). The intensity of this newly appeared band was found to decay with time and finally diminished indicating the unstable nature of the intermediate. The decay was found to follow a pseudo first order kinetics with a rate constant 4.3×10^{-3} s^{-1} at 298 K.

Addition of stoichiometric amount of NO also results in same observation.

In solution FT-IR study, the addition of NO to the acetonitrile solution of complex **2** displayed a new strong stretching frequency at ~1718 cm^{-1} (Fig. 5). The intensity of this band was found to diminish with time suggesting this stretching from an unstable intermediate. This has been assigned as the coordinated nitrosyl

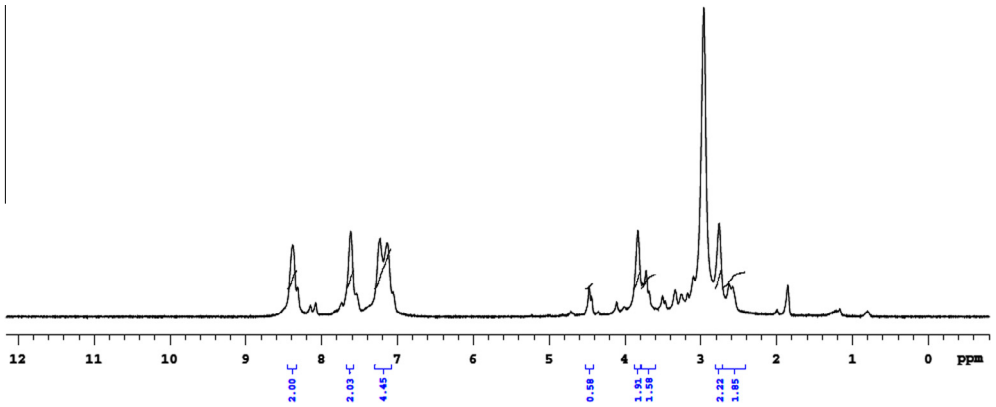

Fig. 7. ^1H NMR spectrum of complex **2** after the reaction of NO under argon atmosphere in CD_3CN.

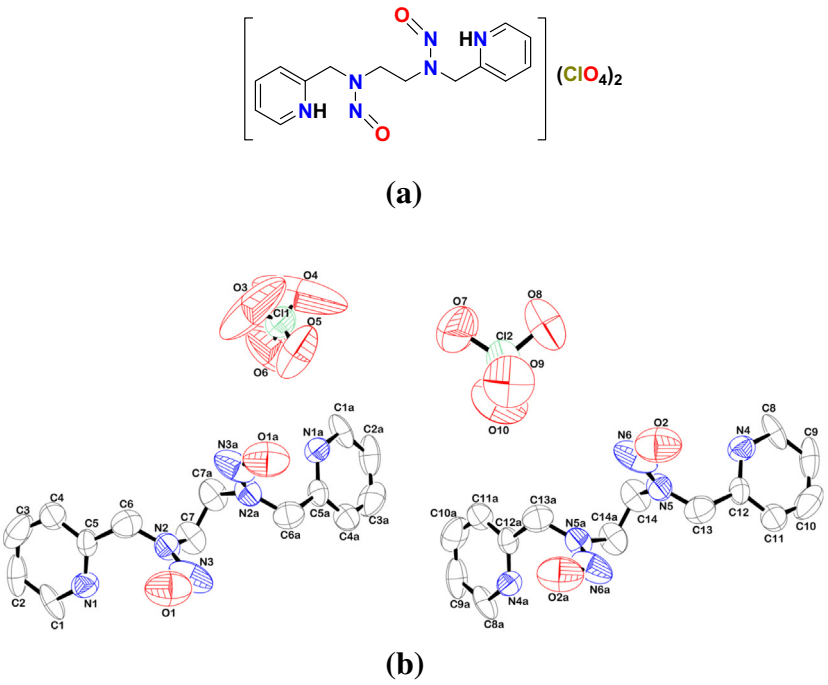

Fig. 8. (a) Modified ligand, L′$(ClO_4)_2$. (b) ORTEP diagram of perchlorate salt of **L′** (50% thermal ellipsoid plot; H-atoms are removed for clarity).

Table 4
Crystallographic data for modified ligand **L′**.

	L′
Formula	$C_{14}H_{18}N_6O_{10}Cl_2$
Mol. wt.	501.24
Crystal system	monoclinic
Space group	*C*2/*c*
T (K)	296(2)
Wavelength (Å)	0.71073
a (Å)	22.837(6)
b (Å)	14.466(6)
c (Å)	13.121(4)
α (°)	90.00
β (°)	103.89(3)
γ (°)	90.00
V (Å^3)	4208(2)
Z	8
Density (mg m^{-3})	1.582
Absorption coefficient (mm^{-1})	0.375
Absorption correction	none
F(000)	2064
Total no. of reflections	1412
Reflections, $I > 2\sigma(I)$	1119
Maximum 2*θ* (°)	25.50
Ranges (*h*, *k*, *l*)	$-27 \leqslant h \leqslant 26$ $-17 \leqslant k \leqslant 16$ $-15 \leqslant l \leqslant 15$
Complete to 2*θ* (%)	98.6
Refinement method	full-matrix least-squares on F^2
GOF (F^2)	0.999
R indices [$I > 2\sigma(I)$]	0.1057
R indices (all data)	0.2977

Table 5
Selected bond length (Å) of **L′**.

	Bond length (Å)		Bond length (Å)
Cl1–O5	1.42(1)	Cl2–O10	1.41(2)
Cl1–O4	1.40(1)	C6–N2	1.45(2)
Cl1–O3	1.40(1)	N2–N3	1.41(2)
Cl1–O6	1.42(2)	N2–C7	1.45(2)
Cl2–O9	1.14(2)	N3–O1	1.25(2)
Cl2–O8	1.36(2)	C13–N5	1.44(2)
Cl2–O7	1.34(2)	O2–N6	1.19(2)

Table 6
Selected bond angles (°) of **L′**.

	Bond angles (°)		Bond angles (°)
O5–Cl1–O4	109.5(7)	O8–Cl2–O10	124(1)
O5–Cl1–O3	114.5(8)	O7–Cl2–O10	96(1)
O5–Cl1–O6	105.2(8)	C6–N2–N3	131(1)
O4–Cl1–O3	109.5(7)	C6–N2–C7	121(1)
O4–Cl1–O6	110.6(8)	N3–N2–C7	108(1)
O3–Cl1–O6	107.4(8)	N2–N3–O1	102(1)
O9–Cl2–O8	114(2)	N4–C12–C11	118(2)
O9–Cl2–O7	124(1)	N4–C12–C13	123(1)
O9–Cl2–O10	106(1)	O2–N6–N5	109(1)
O8–Cl2–O7	92(1)	N6–N5–C14	110(1)

stretching. The EPR study of the intermediate has been done and it was found to be silent (Fig. 6). Thus, intermediate is presumably Mn(II)-mononitrosyl. This has been further supported from the ESI mass spectrum of the intermediate. The peak at 327.112 corresponds to Mn(II)-mononitrosyl (Supporting information). The unstable nature of the intermediate did not allow its isolation of further characterization. It should be noted that the correct assignment of the formal oxidation states of the metal in metal nitrosyls is difficult because of non-innocent nature of NO ligands. NO can exist as NO^+, NO (radical) or NO^-in metal nitrosyl complexes. The observed intermediate is diamagnetic complex of Mn(II) with NO having $\{MnNO\}^6$ configuration according to Enemark–Feltham notation. Thus, it may have Mn(I)-NO^+, Mn(II)-NO or Mn(III)-NO^- configuration. Since the crystal structure is not available, direct comparison of the metric parameters with other reported results to assign the configuration is not possible. On the other hand, the nitrosyl stretching frequency in the intermediate complex appears at ~1718 cm^{-1} in solution FT-IR spectroscopy. This is comparable

with the other reported Mn(II)-nitrosyls having Mn(I)-NO^+ configuration [42–47].

The decomposition of the [Mn(II)-NO] intermediate is resulted in the reduction of Mn(I) and NO^+. The reduction was confirmed by the disappearance of the EPR signal of Mn(II) (Fig. 6).

In addition, the broad ^1H NMR signals of the complex **2** became sharp and well resolved after its reaction with NO (Fig. 7). This has been attributed to the reduction of paramagnetic Mn(II) to diamagnetic Mn(I) by NO.

Although, there is no direct evidence of formation of NO^+ in the reaction mixture, this has been supported by N-nitrosation of the ligand. Nitrosation product, **L′** was isolated from the reaction mixture (Section 2) and characterized using various spectroscopic analyses as well as single crystal x-ray structure determination. The ORTEP diagram of **L′** is shown in Fig. 8. The crystallographic data, selected bond angles and distances are listed in Tables 4–6, respectively. In FT-IR spectrum the N-NO stretching frequency appears at ~1457 cm^{-1} which is in the range of other reported examples.

It should be noted that in cases of Cu(II) complexes of various N-donor ligands, the addition of NO was found to result in [Cu(II)-NO] intermediate prior to the reduction of metal center. This reduction resulted in the N-nitrosation of the ligand frameworks [25–27]. It was observed that while more than one nitrosation sites are available, the nitrosation took place to all the sites [25–27].

Some Cu(II) complexes, depending upon the ligand framework, did not undergo reduction in presence of NO itself. However, addition of base (NaOEt) to the solution of those complexes followed by addition of NO resulted in the reduction of Cu(II) center along with N-nitrosation. In these cases, only mono-nitrosation was observed. For instance, the same ligand was used to prepare Cu(II) complex for NO reactivity study. Although the Cu(II) complex did not react with NO in degassed methanol solution, but in presence of sodium ethoxide as base the reduction was observed with simultaneous N-nitrosation.

It should be noted that addition of sodium ethoxide to the methanol solution of the ligand followed by NO purging leads to insignificant ligand modification (~2–5%).

Mn(II)-nitrosyls, having d^6 configuration according to Enemerk and Feltham notation, have been synthesized with porphyrin, thalocyanins. They were stable and structurally characterized. A series of Mn(II) complexes of N-donor ligands having amide group have been reported to react with NO in acetonitrile solution to afford stable Mn(II)-nitrosyl complex. They were also characterized structurally. The reduction of Mn center in bis-μ-oxo complex by NO was exemplified earlier. This leads to the reductive nitrosylation of the metal ion. However, there is no example of reduction of Mn(II) by NO leading to simultaneous ligand nitrosation.

4. Conclusions

Mn(II) complex, **2**, in acetonitrile solution was found to react with NO to afford unstable Mn(II)-nitrosyl intermediate. The formation nitrosyl intermediate was evidenced by UV–Vis, solution FT-IR, ^1H NMR spectral studies. Subsequently, Mn(II) center in complex **2** was found to undergo reduction to Mn(I) with a simultaneous N-nitrosation of the ligand. The N-nitrosated ligand was isolated and characterized. It should be noted that the corresponding Cu(II) complex of the same ligand in presence of NO was not found to yield Cu(II)-nitrosyl.

Acknowledgements

The authors sincerely thank the Department of Science and Technology, India for financial support; DST-FIST for X-ray diffraction facility. A.K. and S.G. would like to thank CSIR and UGC, India for providing the scholarship.

Appendix A. Supplementary material

Supplementary data (the spectral data of all the compounds) associated with this article can be found, in the online version, at http://dx.doi.org/10.1016/j.ica.2014.12.040.

References

[1] G.B. Richter-Addo, P. Legzdins, Metal Nitrosyls, Oxford University Press, New York, 1992.
[2] M. Feelisch, J.S. Stamler (Eds.), Methods in Nitric Oxide Research, John Wiley and Sons, Chichester, England, 1996.
[3] P.C. Ford, I.M. Lorkovic, Chem. Rev. 102 (2002) 993.
[4] A. Ghosh, Acc. Chem. Res. 38 (2005) 943.
[5] R.J.P. Williams, Chem. Soc. Rev. (1996) 77.
[6] L.J. Ignarro (Ed.), Nitric Oxide: Biology and Pathobiology, Academic Press, San Diego, 2000.
[7] A.R. Butler, D.L. Williams, Chem. Soc. Rev. (1993) 233.
[8] L. Jia, C. Bonaventura, J. Bonaventura, J.S. Stamler, Nature 380 (1996) 221.
[9] J.S. Stamler, Cell 78 (1994) 931.
[10] N.S. Bryan, T. Rassaf, R.E. Maloney, C.M. Rodriguez, F. Saijo, J.R. Rodriguez, M. Feelisch, Proc. Natl. Acad. Sci. U. S. A. 101 (2004) 4308.
[11] B.P. Luchsinger, E.N. Rich, A.J. Gow, E.M. Williams, J.S. Stamler, D.J. Singel, Proc. Natl. Acad. Sci. U. S. A. 100 (2003) 461.
[12] V.K.K. Praneeth, F. Paulat, T.C. Berto, S. De Beer George, C. Nather, C. Sulok, N. Lehnert, J. Am. Chem. Soc. 130 (2008) 15288.
[13] A.V. Soldatova, M. Ibrahim, J.S. Olson, R.S. Czernuszewicz, T.G. Spiro, J. Am. Chem. Soc. 132 (2010) 4614.
[14] I.M. Wasser, S. de Vries, Chem. Rev. 102 (2002) 1201.
[15] M. Hoshino, M. Maeda, R. Konishi, H. Seki, P.C. Ford, J. Am. Chem. Soc. 118 (1996) 5702.
[16] B.O. Fernandez, I.M. Lorkovic, P.C. Ford, Inorg. Chem. 43 (2004) 5393.
[17] D.P. Linder, K.R. Rodgers, J. Banister, G.R.A. Wyllie, M.K. Ellison, W.R. Scheidt, J. Am. Chem. Soc. 126 (2004) 14136.
[18] J. Torres, D. Svistunenko, B. Karlsson, C.E. Cooper, M.T. Wilson, J. Am. Chem. Soc. 124 (2002) 963.
[19] D. Tran, P.C. Ford, Inorg. Chem. 35 (1996) 2411.
[20] D. Tran, B.W. Skelton, A.H. White, L.E. Laverman, P.C. Ford, Inorg. Chem. 37 (1998) 2505.
[21] K. Tsuge, F. DeRosa, M.D. Lim, P.C. Ford, J. Am. Chem. Soc. 126 (2004) 6564.
[22] C. Khin, M.D. Lim, K. Tsuge, A. Iretskii, G. Wu, P.C. Ford, Inorg. Chem. 46 (2007) 9323.
[23] S.D. Pell, J.N. Armor, J. Am. Chem. Soc. 95 (1973) 7625.
[24] M. Sarma, A. Singh, S.G. Gupta, G. Das, B. Mondal, Inorg. Chim. Acta 63 (2010) 63.
[25] M. Sarma, A. Kalita, P. Kumar, A. Singh, B. Mondal, J. Am. Chem. Soc. 132 (2010) 7846.
[26] M. Sarma, B. Mondal, Inorg. Chem. 50 (2011) 3206.
[27] M. Sarma, B. Mondal, Dalton Trans. 41 (2012) 2927.
[28] M. Sarma, V. Kumar, A. Kalita, R.C. Deka, B. Mondal, Dalton Trans. 41 (2012) 9543.
[29] F.G. Quijano, B. Alvarez, R. Radi, Methods Enzymol. 349 (2002) 23.
[30] R. Shimanovich, S. Hannah, V. Lynch, N. Gerasimchuk, T.D. Mody, D. Magda, J. Sessler, J.T. Groves, J. Am. Chem. Soc. 123 (2001) 3613.
[31] Z.N. Zahran, J. Lee, S.S. Alguindigue, M.A. Khan, G.B. Richter-Addo, Dalton Trans. (2004) 44.
[32] A.J. Christopher, A.M. Kirsty, B. Manuel, C.G. Neil, G.J. Nicholas, L.-R. Estefania, O.A. Guy, R.H. Philip, Dalton Trans. (2004) 683.
[33] K. Ghosh, A.A. Eroy-Reveles, B. Avila, T.H. Holman, M.M. Olmstead, P.K. Mascharak, Inorg. Chem. 43 (2004) 2988.
[34] A.C. Merkle, N.L. Fry, P.K. Mascharak, N. Lehnert, Inorg. Chem. 50 (2011) 12192.
[35] K. Ghosh, A.A. Eroy-Reveles, M.M. Olmstead, P.K. Mascharak, Inorg. Chem. 44 (2005) 8469.
[36] K. Tsuge, F. De Rosa, M.D. Lim, P.C. Ford, J. Am. Chem. Soc. 126 (2004) 6564.
[37] SMART, SAINT and XPREP, Siemens Analytical X-ray Instruments Inc., Madison, Wisconsin, USA, (1995).
[38] G.M. Sheldrick, SADABS: Software for Empirical Absorption Correction, University of Gottingen: Institut fur Anorganische Chemieder Universitat, Tammanstrasse 4, D-3400 Gottingen: Germany, 1999. -2003.
[39] G.M. Sheldrick, SHELXS-97, University of Gottingen, Germany, 1997.
[40] L.J. Farrugia, J. Appl. Crystallogr. 30 (1997) 565.
[41] K. Michelsen, Acta Chem. Scand. A31 (1977) 429.
[42] K. Ghosh, A.A. Eroy-Reveles, B. Avila, T.R. Holman, M.M. Olmstead, P.K. Mascharak, Inorg. Chem. 43 (2004) 2988.
[43] L.E. Goodrich, F. Paulat, V.K.K. Praneeth, N. Lehnert, Inorg. Chem. 49 (2010) 6293.
[44] J.H. Enemark, R.D. Feltham, Coord. Chem. Rev. 13 (1974) 339.
[45] W.R. Scheidt, K. Hatano, G.A. Rupprecht, P.L. Piciulo, Inorg. Chem. 18 (1979) 292.
[46] W.M. Coleman, L.T. Taylor, J. Am. Chem. Soc. 100 (1978) 1705.
[47] E. Tangen, J. Conradie, K. Franz, S. Friedle, J. Telser, S.J. Lippard, A. Ghosh, Inorg. Chem. 49 (2010) 2701.